CHEMBIOCHEM

DOI: 10.1002/cbic.200500533

An Efficient Method for the Synthesis of Peptide Aldehyde Libraries Employed in the Discovery of Reversible SARS Coronavirus Main Protease (SARS-CoV M^{pro}) Inhibitors

Samer I. Al-Gharabli,[a, e] Syed T. Ali Shah,[a] Steffen Weik,[a] Marco F. Schmidt,[a, d] Jeroen R. Mesters,[b] Daniel Kuhn,[c] Gerhard Klebe,[c] Rolf Hilgenfeld,[b] and Jörg Rademann*[a, d]

A method for the parallel solid-phase synthesis of peptide aldehydes has been developed. Protected amino acid aldehydes obtained by the racemization-free oxidation of amino alcohols with Dess–Martin periodinane were immobilized on threonyl resins as oxazolidines. Following Boc protection of the ring nitrogen to yield the N-protected oxazolidine linker, peptide synthesis was performed efficiently on this resin. A peptide aldehyde library was designed for targeting the SARS coronavirus main protease, SARS-CoV M^{pro} (also known as $3CL^{pro}$), on the basis of three different reported binding modes and supported by virtual screening. A set of 25 peptide aldehydes was prepared by this method and investigated in inhibition assays against SARS-CoV M^{pro}. Several potent inhibitors were found with IC_{50} values in the low micromolar range. An IC_{50} of 7.5 μM was found for AcNSTSQ-H and AcESTLQ-H. Interestingly, the most potent inhibitors seem to bind to SARS-CoV M^{pro} in a noncanonical binding mode.

Introduction

In November 2002, a novel medical condition emerged in Southern China characterized by symptoms of fever, chills, malaise, headache, cough, and dyspnea, with radiological evidence of pneumonia. The disease was named severe acute respiratory syndrome (SARS), and a novel coronavirus, SARS-CoV, was identified as its causative agent.[1–4] Although the primary SARS epidemic was controlled by the summer of 2003—after affecting about 8500 patients and leaving 800 dead—the re-emergence of this or other new coronaviruses is quite possible and might pose a global public health threat.[5,6] Therefore extensive scientific efforts have been initiated that are directed at novel therapies against pathogenic coronaviruses.

Viral proteases, essential for the maturation of the viral proteome, have been identified as appropriate pharmaceutical targets, as has been reported for human immunodeficiency virus (HIV).[7,8] Similarly, a route to drug design has been opened by the characterization of SARS-CoV M^{pro}. The crystal structure of this enzyme has been determined with a chloromethyl ketone (CMK) inhibitor covalently and irreversibly attached to the active-site cysteine residue (Scheme 3, below).[9] This CMK had been established as an inhibitor of a homologous coronaviral protease (porcine transmissible gastroenteritis virus (TGEV) M^{pro}).[10] Irreversible inhibitors, however, do not yield detailed information on binding affinities and thus are not useful for quantitative determination of structure–activity relationships. This is required for iterative ligand optimization and, potentially, the development of a therapeutic agent.

The work presented here concerns the preparation and identification of reversible SARS-CoV M^{pro} inhibitors. Peptide aldehydes have been established as inhibitors of several classes of proteolytic enzymes[11] including aspartic proteases,[12,13] cysteine proteases,[14,15] and serine proteases.[16,17] Despite their reactivity as electrophiles, a therapeutic potential has also been attributed to peptide aldehydes.[18] Moreover, peptide aldehydes are especially suited for the systematic investigation of structure–activity relationships of protease inhibitors, as they

[a] *Dr. S. I. Al-Gharabli, Dr. S. T. A. Shah, Dr. S. Weik, Dipl.-Biochem. M. F. Schmidt, Prof. Dr. J. Rademann*
Leibniz Institut für Molekulare Pharmakologie (FMP)
Department for Medicinal Chemistry
Robert-Rössle-Straße 10, 13125 Berlin (Germany)
Fax: (+49) 30-94793-280
E-mail: rademann@fmp-berlin.de

[b] *Dr. J. R. Mesters, Prof. Dr. R. Hilgenfeld*
Institut für Biochemie, Center for Structural and Cell Biology in Medicine
Universität Lübeck
Ratzeburger Allee 160, 23538 Lübeck (Germany)

[c] *Dr. D. Kuhn, Prof. Dr. G. Klebe*
Institut für Pharmazeutische Chemie, Philipps-Universität Marburg
Marbacher Weg 6, 35032 Marburg (Germany)

[d] *Dipl.-Biochem. M. F. Schmidt, Prof. Dr. J. Rademann*
Freie Universität Berlin, Institut für Chemie und Biochemie
Takustrasse 3, 14195 Berlin (Germany)

[e] *Dr. S. I. Al-Gharabli*
Current address:
Chemical and Pharmaceutical Engineering, German–Jordanian University
35247 Amman 11180 (Jordan)

mimic the native protease substrate by retaining the hydrogen-bonding pattern of the backbone and addressing the S1, S2, S3,… sites of the enzyme by their amino acid side chains.

A prerequisite for targeting SARS-CoV M^{pro} with peptide aldehydes was a reliable and robust protocol for the parallel synthesis and library preparation of these compounds. The published peptide aldehyde synthesis protocols show limitations in yield, purity, and the ease of product isolation,[11,19,20] so we decided to develop a technique for the synthesis of peptide aldehyde libraries based on an *N*-*tert*-butyl oxycarbonyl (Boc-) protected oxazolidine linker. Various polar and nonpolar polymer supports were assessed to determine the optimimum linker–resin combination. The synthesis technique having been established, a peptide aldehyde library was designed based on a virtual screen of the SARS-CoV M^{pro} active site. The specificities of the active-site pockets were analyzed by using CavBase,[21] and virtual screening was performed with the docking program FlexX.[22] Finally, the library was synthesized by employing the novel linker concept, and the resulting peptide aldehydes were assessed by an enzyme assay.

Results and Discussion

Peptide aldehyde synthesis

Peptide aldehydes are important tools in biochemistry and chemical biology for the inhibition and chemical disabling of proteases. The synthesis of peptide aldehydes has been accomplished by two alternative strategies: by the reduction of protected amino acid derivatives or the oxidation of amino alcohols. Great efforts have been made to optimize these approaches in solution,[23–25] in the solid phase,[20,26–29] and by the use of polymer reagents.[30,31] For the efficient preparation of peptide aldehyde libraries, it would be advantageous to enhance the efficiency of solid-phase peptide synthesis. In particular it would be desirable to have a method that yielded pure peptide aldehydes directly by cleavage from the resin without tedious isolation procedures, such as crystallization or chromatography.[31] Ede and Bray have described the first step for this by introducing a threonine-based oxazolidine linker on "Synphase Crowns", that is, polyethylene carriers grafted to a copolymer of methacrylic acid and dimethylacrylamide.[19] Recently, this linker has been employed with polystyrene in a catch-and-release protocol to purify peptide aldehydes that were first prepared by polymer-supported IBX in solution.[32] However, when we used the oxazolidine linker for peptide synthesis on an immobilized amino acid aldehyde, the method produced disappointingly low yields. Possible explanations for this failure are i) the hydrolytic leaching of aldehyde products during the extended synthesis procedures, ii) the acylation of the oxazolidine nitrogen leading to decreased product release, and iii) inefficient hydrolysis in hydrophobic polystyrene-based resins. We reasoned that protection of the ring nitrogen would provide a way to test the first two possibilities. The third was tested by comparing peptide aldehyde synthesis by using various hydrophobic and hydrophilic (PEG-grafted) resins.

To prepare the protected oxazolidine linker, Fmoc-Thr(trt)-OH was coupled to amino resin **1** by an amide bond (Scheme 1). The resulting polymer-supported Fmoc-threonyl-(trt) amide was deprotected by treatment with 20% piperidine; the trityl group was removed with a mixture of TFA/triisopropylsilane/DCM (1:5:94) at room temperature to yield the deprotected threonyl resin **3**.

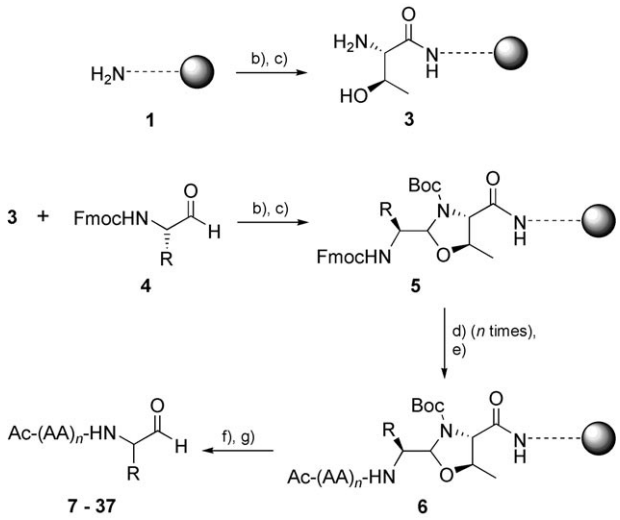

Scheme 1. Preparation of peptide aldehydes. a) Fmoc-Thr(trt)-OH (**2**), TBTU, DIPEA, DMF, RT; 20% piperidine, DMF; b) MeOH/DCM/DMF/AcOH (30:3:2:0.35), RT, 2 h. c) Boc_2O, DIPEA, DCM, 50 °C, 3-4 h. d) Fmoc solid-phase peptide synthesis. e) Ac_2O, pyridine. f) 80% TFA/DCM 30-45 min. g) DCM/MeOH/AcOH/H_2O (12:5:2:1), 3×20 min. AA = amino acids, for details see Table 1.

Fmoc-protected amino acid aldehydes **4** were synthesized from their respective amino alcohols by oxidation with Dess–Martin periodinane. Interestingly, this method led to the racemization-free oxidation of amino alcohols, as reported recently for polymer-supported IBX resin.[32] The oxazolidine formation on resin was selective for aldehydes, with small amounts of alcohols from incomplete oxidation being tolerated well. The coupling of **4** to **3** yielding oxazolidine **5** was investigated under acidic and basic conditions, exhibiting optimum coupling in the presence of AcOH (1%) in MeOH/DCM/DMF. Formation of the oxazolidine moiety was monitored by attenuated total reflection-IR (ATR-IR) spectroscopy and, quantitatively, by the Kaiser test. The yield was quantified by spectrophotometric Fmoc determination. To prevent untimely hydrolysis during the following peptide synthesis and the acylation of the heterocycle, the oxazolidine nitrogen was protected with Boc. The Boc-oxazolidine was fully compatible with the Fmoc strategy and easily deprotected to permit ring cleavage.

After standard peptide chain extension, by using DIC/HOBt couplings, a two-step cleavage protocol was adopted. Side-chain protecting groups including the *N*-Boc-oxazolidine were removed by using an anhydrous mixture of TFA and DCM (8:2). For the Trt-protecting groups, triisopropyl silane (TIPS, 1%) was added to reduce the trityl cation without affecting

the protected aldehyde moiety. In the second cleavage step, mild aqueous acidic conditions were applied to release the deprotected peptide aldehydes from the support. The freed aldehydes were precipitated in diethyl ether after concentration of the cleaving solution and lyophilization by *t*BuOH/H_2O (2:1). Even after only two peptide couplings, a significant difference between the protected and the unprotected oxazolidine was observed. Fmoc-Lys(Fmoc)-Leu-Phe-H (**7**) was obtained in 80% yield on *N*-Boc-protected oxazolidine resin, compared to only 39% on unprotected oxazolidine.

To investigate the impact of the resin type on the efficiency of this method, three resins were selected for the synthesis of peptide aldehydes: aminomethyl polystyrene and two hydrophilic PEG resins, NovaGel and NovaSynTG. The PEG-grafted resins were selected for their good swelling properties in aqueous solvents. NovaSynTG is a tentagel resin with reactive amino groups at the end of long PEG chains ("tentacles"), while Novagel has inert methoxy ether moieties at the end of the PEG chains and a higher loading with aminomethyl polystyrene for linker attachment.

Fmoc-FMGLF-H, Fmoc-GVAIF-H, and Fmoc-APFVF-H (Table 1) were synthesized on these resins according to the method shown in Scheme 1. The purities of the resulting peptide aldehydes were similar, but NovaSynTG and NovaGel resins produced enhanced yields when compared with aminomethyl polystyrene: Fmoc-GVAIF-H was produced in yields of 50, 87, and 82% on aminomethyl polystyrene, NovaGel, and NovaSynTG, respectively. The use of NovaSynTG was compromised by the low loading of the resin, consequently NovaGel was determined to be the optimum resin, providing excellent yields and purities combined with favorable swelling and mechanical properties.

Table 1. Yields for the synthesis of three selected peptides for comparison.

Compounds	Aminomethyl-polystyrene	NovaGel	NovaSynTG
Fmoc-FMGLF-H (**8**)	51%	77%	68%
Fmoc-GVAIF-H (**9**)	50%	87%	82%
Fmoc-APFVF-H (**10a**)	50%	78%	71%

Prepared peptide aldehydes were characterized by HPLC-MS and NMR spectroscopy. In most cases, the HPLC-MS chromatograms displayed one broad peak with a mass-to-charge ratio corresponding to the protonated and the sodiated molecule ion. Additionally, the masses of the hydrated aldehydes were often detected in the same peak. If the side chains of the aldehyde building blocks contained a nucleophile (as in the case of Gln, Lys, or Trp), additional products displaying the masses of dehydrated peptide aldehydes in a broad peak were observed (see Figure 1), corresponding to the formation of cyclized condensation products (Scheme 2). Generally, no peptide-derived by-products were detected in the LC-MS.

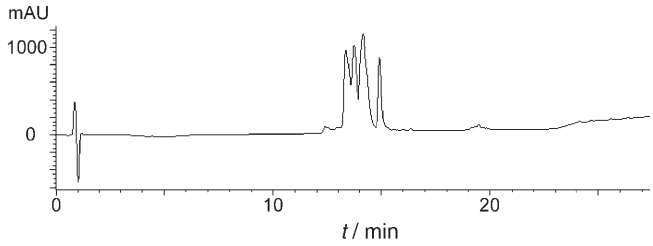

Figure 1. HPLC elution of Ac-DSFDQ-H **37** with an especially "flat" gradient (0–25% acetonitrile over 25 min). Column: Eclipse XDB-C8, Analytical Guard Column, 4.6×12.5 mm, 5 μm (Agilent Technologies); detection at 220 nm; buffer A: 0.1% formic acid in water; buffer B: 0.1% formic acid in ACN. The $[M+H]^+$ signal of **37** was observed in the first two peaks. The two other peaks display the mass of dehydrated peptide aldehyde $[M+H^+-H_2O]$ (see Scheme 2).

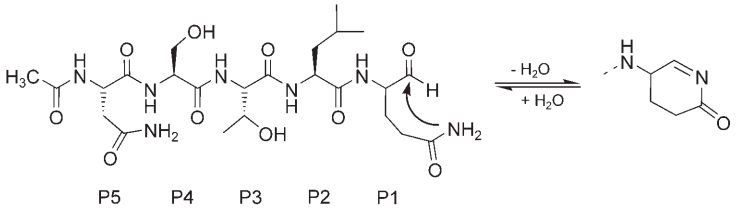

Scheme 2. Peptide aldehydes carrying nucleophilic side chains in P1 resulted in cyclized condensation products, as detected by LC-MS.

Design of a peptide aldehyde library

The cysteine protease SARS-CoV M^{pro} possesses a chymotrypsin-like fold (domains I and II) and a helical domain (domain III). The active site contains a catalytic dyad comprising a cysteine and a histidine residue and is located in a cleft between domains I and II. The protein forms a dimer in the crystal and in solutions of slightly elevated concentrations. It has been shown by X-ray crystallography, with supportive evidence from molecular-dynamics simulations, that the enzyme undergoes pH-dependent conformational changes in its substrate binding site.[9,33] At slightly acidic pH, one of the dimer protomers is in the active, and the other in an inactive conformation. However, when the same crystals are grown at pH 6.0 and then equilibrated at pH 7.6, both monomers are in the active form; this is in agreement with the pH activity profile of the enzyme.[9,33] Comparison of the crystal structures of the main proteases of TGEV M^{pro} [10] and SARS-CoV M^{pro} [9] revealed three possible binding modes for a covalently attached chloromethylketone inhibitor (Scheme 3), thus indicating the structural diversity of the enzyme.

In all three cases, the methylene ketone moiety is covalently attached to Cys145. The P1 glutamine residue is found in the S1 pocket when the protease is in the active conformation (binding modes I and II). However, in the inactive conformation (mode III), the S1 pocket has collapsed and consequently, the P1 glutamine residue is oriented away from the binding site, towards the bulk solvent.

The inhibitor attached to TGEV M^{pro} [10] displays a binding mode with P2, P4, and P5 addressing the respective S pockets, while P3 and P6 are exposed to the solvent (Scheme 3, I). This

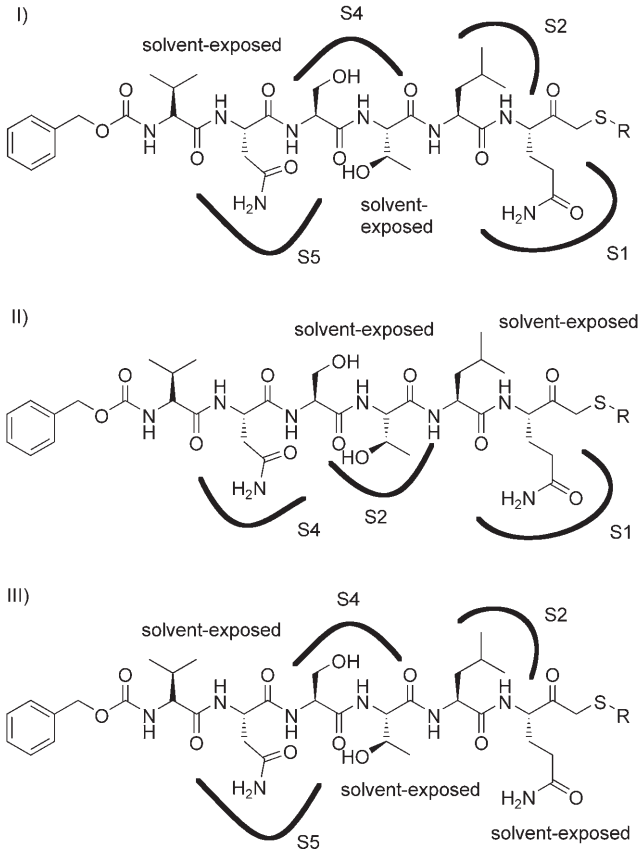

Scheme 3. Binding modes of the irreversible hexapeptidyl CMK inhibitor: I) canonical binding mode observed with TGEV M^{pro} (PDB ID 1P9U);[10] II) noncanonical mode as observed with the active monomer (molecule A) of SARS-CoV M^{pro} (PDB ID 1UK4);[9] and III) binding to the inactive monomer (molecule B) of SARS-CoV M^{pro} (PDB ID 1UK4).[9] No difference in electron density could be observed for the benzyloxycarbonyl (Cbz) protecting group in any of the three crystal structures. Additionally, in the case of both 1UK4 protomers, the terminal valine of the CMK inhibitor has no visible density.

"canonical" binding mode was also observed recently for the SARS-CoV enzyme with irreversible peptide inhibitors other than chloromethylketones.[34,35]

In monomer A of SARS-CoV M^{pro} the CMK inhibitor is in a different side-chain orientation:[9] P2-leucine, P4-serine, and P6-valine do not bind to the respective pockets of the enzyme but remain solvent exposed. Instead, P3-threonine associates with the S2 pocket, and the S4 pocket is occupied by P5-asparagine (Scheme 3, II). This binding mode is most unusual and might be due to the fact that the peptide sequence of the inhibitor corresponds to the N-terminal autocleavage site of the TGEV (but not the SARS-CoV) M^{pro}.[36] On the other hand, it has also been shown that the SARS-CoV enzyme can efficiently cleave a pentadecapeptide corresponding to the autocleavage site of its TGEV homologue.[10]

In the inactive conformation (binding mode III, monomer B, Scheme 3),[9] the peptidyl CMK binds to the target enzyme in a similar way to mode I, with the exception that the P1 glutamine is unable to enter the S1 pocket because this has collapsed.

Based on these structural findings, a modeling study was conducted. We decomposed the binding pocket of the SARS-CoV M^{pro} into the different amino acid recognition subpockets and used these for a homology search.[21,37] Once related subpockets had been found in other proteins, we used the information about the bound ligand fragments present in these structures as a guideline for the design of putative side chains to address the different subpockets of SARS-CoV M^{pro}. By using FlexX a set of 1230 natural and non-natural amino acids from the available chemicals directory (ACD), as well as from the Sigma–Aldrich catalogue, were docked in the S1, S2, and S4 binding pockets. The localization of the peptide backbone as common scaffold was retained as in the crystal structure. For the S1 pocket, glutamine received a high score; for the S2 pocket several aromatic side chains proved superior to the native leucine; for the S4 pocket, various anionic and uncharged polar amino acids received the highest scores.

Based on the analysis of the obtained protein structures and on the results of the virtual screening, a library of peptide aldehydes was designed (Table 2). Starting from the lead AcNSTLQ-H (**13**), derived from the CMK inhibitor, individual positions were permutated while leaving the others unmodified. By this approach we expected to determine, for every position, the side chain with the highest inhibitory activity. The P1 residue was varied (Q, L, K, W, D, and Y) in compounds **13**–**18** in order to challenge the predicted preference for glutamine. For the P2 position, the crystal structures suggested that solvent exposure is possible in binding mode II or the S2 pocket is addressed (in binding modes I and III). Hence, polar H-bonding side chains were tested, and the original L was changed to D and S in compounds **21** and **22**. Compound **19** was included to test the possibility of a "frame-shift" by omitting the P2 amino acid. For the P3 position (which occupies the hydrophobic S2 pocket in SARS-CoV M^{pro}, binding mode II, or solvent-exposed in binding modes I and III), various natural and synthetic hydrophobic side chains were introduced (**23**–**30**). The amino acid residue at the P5 position (binding to S5 in mode I and III,

Table 2. Synthesized peptide aldehydes with IC_{50} values as inhibitors of SARS-CoV main protease.

No.	Sequence	IC_{50} [μM]	No.	Sequence	IC_{50} [μM]
13	AcNSTLQ-H	>500	14	AcNSTLK-H	>500
15	AcNSTLL-H	>500	16	AcNSTLW-H	>500
17	AcNSTLD-H	>50	18	AcNSTLY-H	>50
19	AcNSTQ-H	>500	20	AcNSTAQ-H	>50
21	AcNSTDQ-H	20	22	AcNSTSQ-H	7.5
23	AcNSFLQ-H	>50	24	AcNSHLQ-H	>500
25	AcNS(2,5-difluoro-F)LQ-H	>50	26	AcNS(4-phe-F)LQ-H	>500
27	AcNSWLQ-H	>50	28	AcNS(Naph)LQ-H	>50
29	AcNS(4-Br-F)LQ-H	>50	30	AcNSILQ-H	>50
31	AcFSTLQ-H	>50	32	AcDSTLQ-H	10
33	AcESTLQ-H	7.5	34	AcHSTLQ-H	>50
35	AcQSTLQ-H	>50	36	AcESTSQ-H	>500
37	AcDSFDQ-H	50			

and to S4 in mode II) was varied by using F, D, E, H, and Q, thereby testing the FlexX predictions for S4 (**31**–**35**). Finally two compounds were synthesized with substitutions at multiple positions (**36**, **37**). The P4 position was kept constant in all peptide aldehydes. All target peptide aldehydes were synthesized as described above.

Biochemical evaluation of peptide aldehydes

For the quantitative testing of SARS-CoV M^{pro} inhibitors, an HPLC-based assay was adopted. The substrate SWTSAVLQ↓SGFRKWA (↓ = cleavage site) was cleaved, and the product ratio was determined by HLPC.[33] In the initial screen, all peptide aldehydes were tested with inhibitor (500 μM), substrate (0.5 mM) and enzyme (1.5 μM). Compounds displaying a significant inhibition (< 5% substrate conversion) were then assayed at 50 μM. IC_{50} values were determined for compounds displaying significant inhibition at this concentration.

By following this procedure, four compounds with IC_{50} values at low micromolar concentrations (**21**, **22**, **32**, and **33**) were identified as reversible inhibitors of SARS-CoV M^{pro}. These contained a point mutation at either the P2 or P5 position compared to the lead structure. In compound **21**, the acidic aspartate residue was at least 25 times more active in the P2 position than the native leucine; in **22**, serine at P2 was at least 60 times more active. In the P5 position, aspartate and glutamate (**32** and **33** respectively) were at least 50 times more effective than the native asparagine. At P3 a slight improvement of inhibition was observed for several of the aromatic or hydrophobic side chains (**25**, **27**–**30**). For the P1 position, an increase in activity was observed when the original glutamine aldehyde was replaced by aldehydes derived from aspartic acid or tyrosine (**17** and **18**, respectively). It is interesting that peptide aldehydes containing the hydrophilic residues aspartate or serine at P2 were far better inhibitors than those with the native leucine. In the canonical binding mode I, as well as in the complex with the enzyme in its inactive conformation (mode III), the P2 side chain binds in the hydrophobic S2 pocket, whereas it is solvent exposed in the noncanonical binding mode (II). Since we found hydrophilic residues to be preferred in P2, our data appear to support the unusual binding mode II, as observed in monomer A of the crystal structure of SARS-CoV M^{pro} in complex with the CMK.[9] However, the preference for glutamate or aspartate in position P5 is difficult to explain on the basis of binding mode II, since, in this orientation, the P5 side chain would occupy the S4 site, which is restricted and would not usually accommodate a large side chain such as glutamate.

Aldehydes **36** and **37** were designed in order to investigate the additive effects of the contributions of individual side chains to the inhibitory activity of peptide aldehydes. AcESTSQ-H (**36**) combined the most active side chains at P2 and P5; however, its IC_{50} value was above 500 μM. AcDSFDQ-H (**37**) combined preferable side chains at P2, P3, and P5, yet the inhibitory activity was 50 μM (IC_{50}). Thus, the inhibitory effects of side chains in peptide aldehyde inhibitors for SARS-CoV M^{pro} could not be combined additively. This finding appears to indicate different binding modes for the inhibitors prepared and investigated in this study.

Conclusion

In this article, an efficient approach to the synthesis of peptide aldehyde libraries was developed. It was demonstrated that N-protection of the oxazolidine linker with a Boc-group results in the efficient immobilization of amino aldehydes and allows the subsequent preparation of peptide aldehydes by peptide-synthesis protocols. Yields and purities of the crude peptide aldehydes are significantly improved when compared to those of alternative methods.

This synthetic method was employed to find and optimize peptide aldehyde inhibitors for the SARS coronavirus main protease (SARS CoV M^{pro}), a potential drug target for the treatment of infections by this virus. The peptide aldehyde derived from a published irreversible inhibitor was shown to possess little inhibitory activity ($IC_{50} > 500$ μM). Systematic variation of the P sites of this initial structure revealed two positions with significant potential for improving the binding affinity (P2 and P5), whereas mutations in P1 and P3 yielded only moderately improved inhibitors. The best reversible inhibitors, **22** and **33**, exhibited IC_{50} values at low micromolar concentrations (7.5 μM). Interestingly, the most potent compounds are likely to bind best in the unusual binding mode II (Scheme 3). The increased activities of inhibitors **21** and **22** with hydrophilic (polar or anionic) side chains at P2 (in place of the original leucine) correlate well with the solvent exposition of P2 found in this mode. This differs from the recently described irreversible inhibitors of SARS-CoV M^{pro} that bind in the canonical mode I.[34, 35] Additive inhibitory effects of multiple amino acid substitutions could not be detected in two attempts, a further indication of the diversity of the binding interactions of inhibitors to SARS-CoV M^{pro}

The peptide aldehydes developed in this project are being employed in cocrystallization and soaking experiments with SARS-CoV M^{pro}, in order to find further relevant binding modes at the substrate binding site of this cysteine protease. In parallel, the most active structures are currently being used as starting points for the design of nonpeptide inhibitors of this protease.

Experimental Section

General procedures: Aminomethyl polystyrene, NovaGel and NovaSynTG resins were a gift from Merck Biosciences (Läufelfingen, Switzerland). Fmoc-protected amino acids were purchased from Merck Biosciences and Aldrich (Steinheim, Germany). Solvents were purchased in HPLC grade or freshly distilled before use. All reactions were carried out in plastic syringes.

The NMR measurements were conducted on a Bruker Avance 400 or 600 MHz spectrometer. The IR spectra were measured on a Bruker Vector 22 FT-IR spectrometer employing a split-pea ATR unit. For HPLC-MS analysis, an Agilent system was used with a UV and a ESI-MS detector and a reversed-phase column (Nucleosil 100

C-18, 5 μm, 2×250 mm, Fa. Grom, Herrenberg) operated with acetonitril-water mixtures containing 0.1% formic acid.

Synthetic procedures

Fmoc deprotection: The Fmoc-protected amino functionalized resin (100 mg) was suspended in piperidine (20% in DMF; 2 mL) and shaken for 20 min at RT. The resin was washed with DMF (1×) and the procedure repeated. Finally, the resin was washed thoroughly with DMF (5×), THF (5×) and DCM (5×) and dried under reduced pressure.

Synthesis of threonyl-resin **3**: To a solution of Fmoc-Thr(Trt)-OH (**1**, 5 equiv) and DIPEA (5 equiv) in dry DMF (1 mL), TBTU (5 equiv) was added and the reaction mixture was shaken for 5 min. This pre-activated mixture was then added to the amino resin (100 mg, loading 0.8 mmol g)$^{-1}$ swollen in dry DMF (1 mL) and shaken for 1 h at RT. The resin was filtered and washed thoroughly with DMF (5×), THF (5×), and DCM (5×). Completion of the coupling step was verified with the Kaiser test.[38] Photometric Fmoc-determination indicated quantitative conversion.

Fmoc deprotection of the resin was conducted as described. Then the resin was treated with a mixture of DCM, TIPS, and TFA, (94:5:1, *v/v/v*; 2.5 mL) for 20 min at RT. The deprotecting procedure was repeated three times and the filtered resin was washed with DCM (5×).

Synthesis of Fmoc-amino acid aldehydes ***4***: Fmoc-amino alcohol (5.36 mmol) obtained from Fmoc-amino acid as described in the literature[39] was dissolved in dry DCM (200 mL). Dess–Martin periodinane (12 mmol, 2.2 equiv) was added and dissolved almost completely followed by water addition (200 μL, 11.1 mmol). The reaction was monitored by TLC and was completed after 1 h stirring. The reaction mixture was diluted with diethylether (150 mL) and then with 80% bicarbonate solution (150 mL) containing sodium thiosulfate-pentahydrate (60.12 mmol) and stirred for further 30 min. The aqueous phase was extracted with Et_2O (300 mL). The combined organic phases were washed with saturated bicarbonate, water (2×), and brine (2×) and dried over Na_2SO_4. Solvents were removed in vacuo. Fmoc amino acid aldehydes were obtained in 99% yield and characterized by HPLC-MS, NMR, and optical rotation.

Optical rotations that have not been reported in the literature or are higher than the highest reported literature value:

4a: Fmoc-Phe-H: $[\alpha]_D^{20} = +51.2^\circ$

4b: Fmoc-Trp(Boc)-H: $[\alpha]_D^{20} = +14.7^\circ$

4c: Fmoc-Gln(Trt)-H: $[\alpha]_D^{20} = +15.5^\circ$

4d: Fmoc-Leu-H: $[\alpha]_D^{20} = +21.3^\circ$

4e: Fmoc-Tyr(*t*Bu)-H: $[\alpha]_D^{20} = +30.5^\circ$

Synthesis of resin-bound oxazolidines ***5***: The deprotected threonyl-resin (100 mg) was suspended in a mixture of MeOH, DCM, DMF, and AcOH, (30:3:2:0.35, *v/v/v/v*; 2 mL). Fmoc-amino acid aldehyde **4** (5 equiv) was added to the resin and shaken for 3 h at RT under inert atmosphere. Completion of the coupling step was verified with the Kaiser test[38] and the filtered resin was thoroughly washed with DMF (5×), THF (5×), and DCM (5×).

Boc protection of amine moiety in the oxazolidine ring: To resin-bound oxazolidines (100 mg) suspended in DCM (1 mL), a mixture of Boc_2O (5 equiv), DIPEA (1 equiv) diluted in DCM (1 mL) was added. After 3 h shaking, the resin was collected by filtration and washed thoroughly with DMF (5×), THF (5×), and DCM (5×). The completeness of protection was monitored by IR and the chloranil test. The loading of the resin was determined by the Fmoc UV assay.

Peptidyl oxazolidine resin 6 A solution of Fmoc-amino acid (5 equiv) and HOBt (5 equiv) in dry DMF (1 mL) was added to the polymer-bound Fmoc-deprotected oxazolidines **5** (100 mg) swollen in DMF (1 mL). DIC (5 equiv) was added to the suspension and shaken for 1 h at RT. The resin was filtered and washed thoroughly with DMF (5×), THF (5×), and DCM (5×).

Peptide aldehydes ***7–37***: To remove the Boc-protecting group and tert-butyl protecting groups the resin-bound peptidyl oxazolidines **5** (100 mg) were treated with a mixture of TFA and dry DCM (80:20, *v/v*, 2.5 mL) for 0.5 h at RT. The resin was washed with DCM (5×).

A mixture of DCM, MeOH, AcOH, and H_2O (12:5:2:1, *v/v/v/v*) was added to the deprotected resin-bound peptide aldehyde **6** and shaken for 20 min at RT. The resin was filtered off and washed with DCM (2×). The release procedure was repeated three times and the combined filtrates were concentrated under reduced pressure to about 500 μL volume. The products were precipitated by adding cold diethylether and collected by centrifugation. The peptide aldehydes were lyophilized from a solution of tert-butyl alcohol/H_2O (3:1, *v/v*). The products were characterized using HPLC-ESI-MS and NMR spectroscopy.

Fmoc-FMGLF-H (8): for yields on different resins see Table 1. ESI/MS: calcd [M = $C_{46}H_{53}N_5O_7S$] 820.0; found *m/z* 843.2 [*M*+Na]$^+$.

Fmoc-GVAIF-H (9): for yields on different resins see Table 1. ESI/MS: calcd [M = $C_{40}H_{49}N_5O_7$] 711.0; found *m/z* 734.3 [*M*+Na]$^+$.

Fmoc-APFVF-H (10a): for yields on different resins see Table 1. ESI/MS: calcd [M = $C_{46}H_{51}N_5O_7$] 785.0; found *m/z* 808.1 [*M*+Na]$^+$.

Ac-APFVF-H (10b): ^{1}H NMR (300 MHz, [D$_6$]DMSO): $\delta = 0.87$ (m, 6H; CH(C*H*$_3$)$_2$), 1.24 (d, $^3J = 6.0$ Hz, 3H; CHC*H*$_3$), 1.80 (m, 2H; proline, NCH$_2$C*H*$_2$C*H*$_2$CH), 1.91 (s, 3H; C*H*$_3$CO), 1.93 (m, 3H; proline, NCH$_2$C*H*$_2$CH$_2$CH, C*H*(CH$_3$)$_2$), 2.63, 3.04 (m, 4H; (C*H*$_2$Ph)$_2$), 3.64 (m, 2H; proline. NC*H*$_2$CH$_2$CH$_2$CH), 4.25 (m, 1H; CH$_3$C*H*), 4.35 (m, 1H; CHOC*H*), 4.40 (m, 1H; C*H*CH(CH$_3$)$_2$), 4.55, 4.59 (m, 2H; C*H*CH$_2$Ph; proline C*H*), 7.15–7.35 (m, 11H; (CH$_2$C$_6$*H*$_5$)$_2$, CH$_3$CON*H*), 7.66 (m, 1H; proline CON*H*), 8.29 (m, 1H; N*H*CHCH(CH$_3$)$_2$), 8.40 (m, 1H; CHOCHN*H*), 9.50 (s, 1H; C*H*O), ESI/MS: calcd [M = $C_{46}H_{51}N_5O_7$] 605.3; found *m/z* 606.1 [*M*+H]$^+$.

AcNSTLQ-H (13): resin loading before cleavage: 0.27 mmol g^{-1}, yield: 85%. ESI/MS: calcd [M = $C_{24}H_{41}N_7O_{10}$] 587.0; found *m/z* 570.3 [*M*+H$^+$−H$_2$O].

AcNSTLK-H (14): ESI/MS: calcd [M = $C_{25}H_{45}N_7O_9$] 587.0; found *m/z* 570.3 [*M*+H$^+$−H$_2$O].

AcNSTLL-H (15): ESI/MS: calcd [M = $C_{25}H_{44}N_6O_9$] 572.0; found *m/z* 573.3 [*M*+H]$^+$.

AcNSTLW-H (16): ESI/MS: calcd [M = $C_{30}H_{43}N_7O_9$] 645.0; found *m/z* 628.3 [*M*+H$^+$−H$_2$O].

AcNSTLD-H (17): ESI/MS: calcd [M = $C_{23}H_{38}N_6O_{11}$] 574.0; found *m/z* 597.1 [*M*+Na]$^+$.

AcNSTLY-H (18): ESI/MS: calcd [M = $C_{28}H_{42}N_6O_{10}$] 622.0; found *m/z* 623.3 [*M*+H]$^+$.

AcNSTQ-H (19): resin loading before cleavage: 0.24 mmol g^{-1}, yield: 87%.ESI/MS: calcd [M = $C_{18}H_{30}N_6O_9$] 474.0; found *m/z* 457.2 [*M*+H$^+$−H$_2$O].

AcNSTAQ-H (20): resin loading before cleavage: 0.29 mmol g^{-1}, yield: 65%.ESI/MS: calcd [M = $C_{21}H_{35}N_7O_{10}$] 545.0; found *m/z* 528.3 [*M*+H$^+$−H_2O].

AcNSTDQ-H (21): resin loading before cleavage: 0.23 mmol g^{-1}, yield: 60%.ESI/MS: calcd [M = $C_{22}H_{35}N_7O_{12}$] 589.0; found *m/z* 572.2 [*M*+H$^+$−H_2O].

AcNSTSQ-H (22): resin loading before cleavage: 0.29 mmol g^{-1}, yield: 76%. ESI/MS: calcd [M = $C_{21}H_{35}N_7O_{11}$] 561.0; found *m/z* 544.2 [*M*+H$^+$−H_2O].

AcNSFLQ-H (23): ESI/MS: calcd [M = $C_{29}H_{43}N_7O_9$] 633.0; found *m/z* 638.1 [*M*+Na$^+$−H_2O].

AcNSHLQ-H (24): ESI/MS: calcd [M = $C_{26}H_{41}N_9O_9$] 623.0; found *m/z* 606.2 [*M*+H$^+$−H_2O].

AcNS(2,5-difluoro-F)LQ-H (25): ESI/MS: calcd [M = $C_{29}H_{41}F_2N_7O_9$] 669.0; found *m/z* 652.2 [*M*+H$^+$−H_2O].

AcNS(4-phenyl-F)LQ-H (26): ESI/MS: calcd [M = $C_{35}H_{47}N_7O_9$] 709.0; found *m/z* 692.3 [*M*+H$^+$−H_2O].

AcNSWLQ-H (27): ESI/MS: calcd [M = $C_{31}H_{44}N_8O_9$] 672.0; found *m/z* 655.3[*M*+H$^+$−H_2O].

AcNS(Naph)LQ-H (28): ESI/MS: calcd [M = $C_{33}H_{45}N_7O_9$] 683.0; found *m/z* 688.2 [*M*+Na$^+$−H_2O].

AcNS(4-Br-F)LQ-H (29): ESI/MS: calcd [M = $C_{29}H_{42}BrN_7O_9$] 712.0; found *m/z* 695.2 [*M*+H$^+$−H_2O].

AcNSILQ-H (30): ESI/MS: calcd [M = $C_{26}H_{45}N_7O_9$] 599.0; found *m/z* 582.3 [*M*+H$^+$−H_2O].

AcFSTLQ-H (31): resin loading before cleavage: 0.38 mmol g^{-1}, yield: 91%. ESI/MS: calcd [M = $C_{29}H_{44}N_6O_9$] 620.0; found *m/z* 603.3 [*M*+H$^+$−H_2O].

AcDSTLQ-H (32): resin loading before cleavage: 0.28 mmol g^{-1}, yield: 89%. ESI/MS: calcd [M = $C_{24}H_{40}N_6O_{11}$] 588.0; found *m/z* 571.2 [*M*+H$^+$−H_2O].

AcESTLQ-H (33): resin loading before cleavage: 0.41 mmol g^{-1}, yield: 75%.ESI/MS: calcd [M = $C_{25}H_{42}N_6O_{11}$] 602.0; found *m/z* 585.3 [*M*+H$^+$−H_2O].

AcHSTLQ-H (34): resin loading before cleavage: 0.34 mmol g^{-1}, yield: 85%.ESI/MS: calcd [M = $C_{26}H_{42}N_8O_9$] 610.0; found *m/z* 593.1 [*M*+H$^+$−H_2O].

AcQSTLQ-H (35): resin loading before cleavage: 0.42 mmol g^{-1}, yield: 71%. ESI/MS: calcd [M = $C_{25}H_{43}N_7O_{10}$] 601.0; found *m/z* 584.3 [*M*+H$^+$−H_2O].

AcESTSQ-H (36): ESI/MS: calcd [M = $C_{22}H_{36}N_6O_{12}$] 576.0; found *m/z* 559.3 [*M*+H$^+$−H_2O].

AcDSFDQ-H (37): ESI/MS: calcd [M = $C_{27}H_{36}N_6O_{12}$] 636.0; found *m/z* 619.2 [*M*+H$^+$−H_2O].

Bioassay SARS-CoV M^{pro}: Enzyme activity was measured by using a peptide-cleavage assay conducted at pH 7.0.[33] with the peptide substrate NH_2-SWTSAVLQ↓SGFRKWA-COOH. Cleavage reaction mixtures (SARS-CoV M^{pro} (1.5 μM), Na_2HPO_4 (20 mM, pH 7), NaCl (200 mM), EDTA (1 mM), and substrate (0.5 mM) in a total volume of 60 μL) were incubated at 298 K. Aliquots of the reaction mixture were removed at 90 min intervals, added to an equal volume of trifluoroacetic acid (2%), immersed in liquid N_2, and stored at 193 K. The samples were centrifuged (15000 *g*, 10 min) before analysis by reversed-phase HPLC on a C18 column (3.9×150 mm). Cleavage products were resolved in a 15 min, 5–60% linear gradient of acetonitrile in trifluoroacetic acid (0.1%). The absorbance was determined at 280 nm, and peak areas were calculated by integration.

Acknowledgements

We wish to thank Merck Biosciences, Boehringer Ingelheim Pharma, and the DFG (Ra895/2-3, Hi611/4-1) for supporting this work. R.H. thanks the Fonds der Chemischen Industrie for continuous support.

Keywords: aldehydes · cysteine proteases · inhibitors · SARS · solid-phase synthesis · viruses

[1] D. A. Brian, R. S. Baric in *Current Topics in Microbiology and Immunology, Vol. 287* (Ed.: L. Enjuanes), Springer, Heidelberg **2005**, pp. 1–30.
[2] T. Imai, K. Takahashi, T. Hoshuyama, N. Hasegawa, M. K. Lim, D. Koh, *Emerging Infect. Dis.* **2005**, *11*, 404–410.
[3] P. Daszak, G. M. Tabor, A. M. Kilpatrick, J. Epstein, R. Plowright, *Ann. N. Y. Acad. Sci.* **2004**, *1026*, 1–11.
[4] D. A. Groneberg, R. Hilgenfeld, P. Zabel, *Respir. Res.* **2005**, *6*, 8–31.
[5] E. G. Baumeister, A. P. Lewis, J. P. Bozzini, V. L. Savy, *Medicina (Buenos Aires, Argent)* **2005**, *65*, 36–40.
[6] R. A. M. Fouchier, T. Kuiken, M. Schutten, G. van Amerongen, J. van Doornum, B. G. van den Hoogen, M. Peiris, W. Lim, K. Stöhr, A. D. M. E. Osterhaus, *Nature* **2003**, *423*, 240.
[7] R. Wolkowicz, G. P. Nolan, *Gene Ther.* **2005**, *12*, 467–476.
[8] M. A. Winters, T. C. Merigan, *Antimicrob. Agents Chemother.* **2005**, *49*, 2575–2582.
[9] H. Yang, M. Yang, Y. Ding, Y. Liu, Z. Lou, Z. Zhou, L. Sun, Mo. L, S. Ye, H. Pang, G. F. Gao, K. Anand, M. Bartlam, R. Hilgenfeld, Z. Rao, *Proc. Natl. Acad. Sci. USA* **2003**, *100*, 13190–13195.
[10] K. Anand, J. Ziebuhr, P. Wadhwani, J. R. Mesters, R. Hilgenfeld, *Science* **2003**, *300*, 1763–1767.
[11] J. A. Fehrentz, M. Paris, A. Heitz, J. Velek, C. F. Liu, F. Winternitz, J. Martinez, *Tetrahedron Lett.* **1995**, *36*, 7871–7874.
[12] E. Sarubbi, P. F. Seneci, M. R. Angelastro, N. P. Peet, M. Denaro, K. Islam, *FEBS Lett.* **1993**, *319*, 253–256.
[13] J. A. Fehrentz, A. Heitz, B. Castro, C. Cazaubon, D. Nisato, *FEBS Lett.* **1984**, *167*, 273–276.
[14] N. A. Thornberry, H. G. Bull, J. R. Calaycay, K. T. Chapman, A. D. Howard, M. J. Kostura, D. K. Miller, S. M. Molineaux, J. R. Weidner, J. Aunins, K. O. Elliston, J. M. Ayala, F. J. Casano, J. Chin, G. J. F. Ding, L. A. Egger, E. P. Gaffney, G. Limjuco, O. C. Palyha, S. M. Raju, A. M. Rolando, J. P. Salley, T. T. Yamin, T. D. Lee, J. E. Shively, M. Maccross, R. A. Mumford, J. A. Schmidt, M. J. Tocci, *Nature* **1992**, *356*, 768–774.
[15] T. L. Graybill, R. E. Dolle, C. T. Helaszek, R. E. Miller, M. A. Ator, *Int. J. Pept. Protein Res.* **1994**, *44*, 173–182.
[16] R. M. McConnell, J. L. York, D. Frizzell, C. Ezell, *J. Med. Chem.* **1993**, *36*, 1084–1089.
[17] E. Barabás, E. Széll, S. Bajusz, *Blood Coagulation Fibrinolysis* **1993**, *4*, 243–248.
[18] A. Damodaran, R. B. Harris, *J. Protein Chem.* **1995**, *14*, 431–440.
[19] K. Kawamura, S. Kondo, K. Maeda, H. Umezawa, *Chem. Pharm. Bull.* **1969**, *17*, 1902–1909.
[20] T. Someno, S. I. Ishii, *Chem. Pharm. Bull.* **1986**, *34*, 1748–1754.
[21] A. M. Murphy, R. Dagnino, P. L. Vallar, A. J. Trippe, S. L. Sherman, R. H. Lumpkin, S. Y. Tamura, T. R. Webb, *J. Am. Chem. Soc.* **1992**, *114*, 3156–3157.
[22] C. Gros, C. Boulègue, N. Galeotti, G. Niel, P. Jouin, *Tetrahedron* **2002**, *58*, 2673–2680.
[23] D. Lelièvre, O. Turpin, S. El Kazzouli, A. Delmas, *Tetrahedron* **2002**, *58*, 5525–5533.
[24] O. Melnyk, M. Bossus, D. David, C. Rommens, H. Gras-Masse, *J. Pept. Res.* **1998**, *52*, 180–184.
[25] J. Rademann, M. Meldal, K. Bock, *Chem. Eur. J.* **1999**, *5*, 1218–1225.

[26] G. Sorg, A. Mengel, G. Jung, J. Rademann, *Angew. Chem.* **2001**, *113*, 4532 – 4535; *Angew. Chem. Int. Ed.* **2001**, *40*, 4395 – 4397.
[27] C. Agami, F. Couty, C. Lequesne, *Tetrahedron Lett.* **1994**, *35*, 3309 – 3312.
[28] N. J. Ede, A. M. Bray, *Tetrahedron Lett.* **1997**, *38*, 7119 – 7122.
[29] S. Schmitt, D. Kuhn, G. Klebe, *J. Mol. Biol.* **2002**, *323*, 387 – 406.
[30] M. Rarey, B. Kramer, T. Lengauer, G. Klebe, *J. Mol. Biol.* **1996**, *261* 470 – 489
[31] G. Sorg, B. Thern, O. Mader, J. Rademann, G. Jung, *J. Pept. Sci.* **2005**, *11*, 142 – 152.
[32] J. Tan, K. H. G. Verschueren, K. Anand, J. Shen, M. Yang, Y. Xu, Z. Rao, J. Bigalke, B. Heisen, J. R. Mesters, K. Chen, X. Shen, H. Jiang, R. Hilgenfeld, *J. Mol. Biol.* **2005**, *354*, 25 – 40.
[33] H. Yang, W. Xie, X. Xue, K. Yang, J. Ma, W. Liang, Q. Zhao, Z. Zhou, D. Pei, J. Ziebuhr, R. Hilgenfeld, K. Y. Yuen, L. Wong, G. Gao, S. Chen, Z. Chen, D. Ma, M. Bartlam, Z. Rao, *PLoS Biology* **2005**, *3*, e324.
[34] T. W. Lee, M. M. Cherney, C. Huitema, J. Liu, K. E. James, J. C. Powers, L. D. Eltis, M. N. James, *J. Mol. Biol.* **2005**, *353*, 1137 – 1151.
[35] K. Anand, H. Yang, M. Bartlam, Z. Rao, R. Hilgenfeld in *Coronaviruses, with Special Emphasis on First Insights Concerning SARS* (Eds.: A. Schmidt, M. H. Wolff, O. Weber), Birkhäuser, Basel, **2005**, pp. 173 – 199.
[36] D. Kuhn, N. Weskamp, S. Schmitt, E. Hüllermeyer, G. Klebe, *J. Mol. Biol.* **2006**, in press.
[37] E. Kaiser, R. L. Colescot, C. D. Bossinge, P. I. Cook, *Anal. Biochem.* **1970**, *34*, 595.
[38] A. Boeijen, J. van Ameijde, R. M. J. Liskamp, *J. Org. Chem.* **2001**, *66*, 8454 – 8462.
[39] J. C. Kappel, G. Barany, *J. Pept. Sci.* **2005**, *11*, 525 – 535.

Received: December 12, 2005
Published online on May 10, 2006

